

PERPENDICULAR DIFFUSION OF ENERGETIC PARTICLES IN NOISY REDUCED MAGNETOHYDRODYNAMIC TURBULENCE

A. SHALCHI AND M. HUSSEIN

Department of Physics and Astronomy, University of Manitoba, Winnipeg, Manitoba R3T 2N2, Canada;
andream4@yahoo.com, m_hussein@physics.umanitoba.ca

Received 2014 May 5; accepted 2014 August 11; published 2014 September 24

ABSTRACT

A model for noisy reduced magnetohydrodynamic turbulence was recently proposed. This model was already used to study the random walk of magnetic field lines. In the current article we use the same model to investigate the diffusion of energetic particles across the mean magnetic field. To compute the perpendicular diffusion coefficient, two analytical theories are used, namely, the Non-Linear Guiding Center theory and the Unified Non-Linear Transport (UNLT) theory. It is shown that the two theories provide different results for the perpendicular diffusion coefficient. We also perform test-particle simulations for the aforementioned turbulence model. We show that only the UNLT theory describes perpendicular transport accurately, confirming that this is a powerful tool in diffusion theory.

Key words: diffusion – magnetic fields – turbulence

1. INTRODUCTION

In this paper we explore perpendicular diffusion of energetic particles such as cosmic rays due to the interaction with turbulent magnetic fields. The perpendicular diffusion coefficient is one of the elements entering the cosmic ray transport equation. In general, the diffusion of energetic particles is important to understand different processes in space and astrophysics. Some examples discussed more recently in the literature are

1. the acceleration of particles due to turbulence (see Lynn et al. 2014);
2. shock acceleration at interplanetary shocks (see Li et al. 2012; Wang et al. 2012);
3. solar modulation studies (see Alania et al. 2013; Engelbrecht & Burger 2013; Manuel et al. 2014; Potgieter et al. 2014);
4. the motion of cosmic rays in our own and in external galaxies (see Buffie et al. 2013; Berkhuysen et al. 2013);
5. diffusive shock acceleration in supernova remnants (see Ferrand et al. 2014).

Here, we explore perpendicular transport analytically and numerically for a specific turbulence model.

In the solar system, for instance, energetic particles interact with the solar wind plasma and, therefore, are scattered. Spatial diffusion is mainly caused by turbulent magnetic fields $\delta\mathbf{B}$. In addition to such fields we also find an ordered magnetic field \mathbf{B}_0 which breaks the symmetry of the considered physical system. Therefore, we have to distinguish between diffusion of particles along and across the ordered magnetic field, which can also be called the mean magnetic field.

Diffusion across this field, also called perpendicular diffusion, is very difficult to describe analytically (see Shalchi 2009 for a review). More than a decade ago some progress was achieved with the development of the Non-Linear Guiding Center (NLGC) theory of Matthaeus et al. (2003); more recently the Unified Non-Linear Transport (UNLT) theory was presented in Shalchi (2010). UNLT contains the NLGC theory, the field line transport theory of Matthaeus et al. (1995), and the quasi-linear theory of Jokipii (1966) as special limits. Furthermore, the theory automatically provides a subdiffusive result for

magnetostatic slab turbulence in agreement with the theory of reduced dimensionality (see Jokipii et al. 1993; Jones et al. 1998) and computer simulations (see, e.g., Qin et al. 2002).

In order to compute the perpendicular diffusion coefficient based on the aforementioned transport theories, one has to employ a certain turbulence model. Previous models for which the perpendicular diffusion coefficient was calculated are the slab/two-dimensional (2D) composite model (sometimes called the two-component model) and the Goldreich–Sridhar model (see, e.g., Tautz & Shalchi 2011; Shalchi 2013a). In this paper we employ another model which was recently proposed, namely, the noisy reduced magnetohydrodynamic (NRMHD) turbulence model of Ruffolo & Matthaeus (2013).

Here, we explore perpendicular diffusion in NRMHD turbulence analytically and numerically. By doing this we try to achieve the following:

1. showing how the field line random walk (FLRW) limit with the correct field line diffusion coefficient can be obtained from the UNLT theory.
2. obtaining for the first time the perpendicular diffusion coefficient of energetic particles for NRMHD turbulence.
3. testing the validity of NLGC and UNLT theories by comparing them with test-particle simulations in order to check our understanding of perpendicular diffusion.

The remainder of this paper is organized as follows. In Section 2, we briefly present the NLGC theory as well as the UNLT theory. A discussion of the NRMHD turbulence model is given in Section 3. In Section 4, we compute the perpendicular diffusion coefficient analytically and, in Section 5, we use simulations to test our analytical findings. We end with a short summary and some conclusions in Section 6.

2. ANALYTICAL THEORIES FOR PERPENDICULAR DIFFUSION

An analytical description of perpendicular diffusion is difficult (see Shalchi 2009 for a review) since the quasi-linear approximation is only valid in exceptional cases. A promising theory was proposed by Matthaeus et al. (2003), which is called the NLGC theory. This theory was compared with test-particle

simulations and solar wind observations and agreement was often found (see, e.g., Matthaeus et al. 2003; Bieber et al. 2004). However, there are also problems with the theory such as the fact that the theory does not provide subdiffusive transport for slab turbulence¹ (see Shalchi 2009; Tautz & Shalchi 2011). Therefore, different extensions of the NLGC theory were proposed. One example is the Extended Non-Linear Guiding Center proposed by Shalchi (2006). This theory was explicitly developed to handle perpendicular transport in slab/2D composite turbulence and provides the correct subdiffusive behavior for the pure slab case. Alternative approaches were proposed thereafter (see, e.g., Qin 2007; Ghilea et al. 2011; Ruffolo et al. 2012). All these approaches are basically extensions of the original NLGC theory.

A very different approach was proposed by Shalchi (2010), namely the UNLT theory. The main problem in analytical theories for perpendicular diffusion is the emergence of fourth order correlation functions. In the NLGC theory and the aforementioned extensions, such fourth order correlations are approximated by a product of two second order correlations. The second order correlations are then approximated by different models such as a diffusion model (Matthaeus et al. 2003; Shalchi 2006) or a random ballistic model (Ghilea et al. 2011; Ruffolo et al. 2012). The UNLT theory is based on the direct evaluation of fourth order correlations by using the (pitch-angle dependent) Fokker–Planck equation. The UNLT theory correctly describes subdiffusive transport in slab turbulence and contains the correct FLRW limit without specifying the turbulence properties² (see, e.g., Shalchi 2014). It also contains the NLGC theory and the field line diffusion theory of Matthaeus et al. (1995) as special limits, hence the name UNLT theory is justified.

In the current paper, we compute the perpendicular diffusion coefficient based on the NLGC theory and the UNLT theory. In the following two paragraphs, these two theories are discussed.

2.1. The Non-Linear Guiding Center Theory

In Matthaeus et al. (2003), the so-called NLGC theory was derived. The latter theory is based on several assumptions leading to the following nonlinear integral equation for the perpendicular diffusion coefficient:

$$\kappa_{\perp} = \frac{a^2 v^2}{3B_0^2} \int d^3k \frac{P_{xx}(\mathbf{k})}{\kappa_{\parallel} k_{\parallel}^2 + \kappa_{\perp} k_{\perp}^2 + v/\lambda_{\parallel}}. \quad (1)$$

Here we used the wavevector \mathbf{k} , the magnetic correlation tensor

$$P_{mn}(\mathbf{k}) = \langle \delta B_m(\mathbf{k}) \delta B_n^*(\mathbf{k}) \rangle, \quad (2)$$

the parallel diffusion coefficient of the particle κ_{\parallel} , the parallel mean free path $\lambda_{\parallel} = 3\kappa_{\parallel}/v$, the mean magnetic field B_0 , and the particle speed v . We also used the parameter a^2 , which is related to the probability that the particle is tied to a single magnetic field line. Equation (1) was derived under the assumption that $\delta B_z \ll B_0$ and that the turbulence is static.

¹ We want to emphasize that subdiffusive behavior is an aspect of pure magnetostatic slab turbulence and for this specific model, NLGC theory does not work. For a slab/2D composite model, however, diffusion should be recovered. For two-dimensional (2D) turbulence, NLGC theory should be valid. It is not our intention to criticize the slab/2D model or any other model of magnetic turbulence.

² The UNLT theory contains the correct FLRW limit and the Matthaeus et al. (1995) theory. The NLGC theory does not contain this limit. However, it was shown before (see, e.g., Minnie et al. 2009) that for 2D turbulence and certain forms of the spectrum, the FLRW limit can be obtained.

2.2. The UNLT Theory

Because the NLGC theory is problematic in some cases, Shalchi (2010) derived the so-called UNLT theory. UNLT still provides a nonlinear integral equation for the perpendicular diffusion coefficient like the NLGC theory. However, it contains different terms in the denominator,³

$$\kappa_{\perp} = \frac{a^2 v^2}{3B_0^2} \int d^3k \frac{P_{xx}(\mathbf{k})}{F(k_{\parallel}, k_{\perp}) + (4/3)\kappa_{\perp} k_{\perp}^2 + v/\lambda_{\parallel}}, \quad (3)$$

where we have used

$$F(k_{\parallel}, k_{\perp}) = \frac{(2vk_{\parallel}/3)^2}{(4/3)\kappa_{\perp} k_{\perp}^2} \equiv \frac{v^2 k_{\parallel}^2}{3\kappa_{\perp} k_{\perp}^2}. \quad (4)$$

The parameters used here are the same as in Equation (1). Although the integral equation (Equation (3)) has some similarities with Equation (1), the two theories provide different results in the general case (see Tautz & Shalchi 2011).

3. NOISY REDUCED MAGNETOHYDRODYNAMIC TURBULENCE

Ruffolo & Matthaeus (2013) proposed the NRMHD turbulence model. All details can be found in the aforementioned paper. In the following, we discuss some aspects of this model and its relation to 2D turbulence.

3.1. The Correlation Tensor for NRMHD Turbulence

In the following, we discuss the magnetic correlation tensor (Equation (2)) for the NRMHD model. According to Ruffolo & Matthaeus (2013), the two relevant components of the magnetic correlation tensor have the form

$$P_{xx}(\mathbf{k}) = \frac{1}{4\pi K} k_y^2 A(k_{\perp}) \begin{cases} 1 & \text{if } |k_{\parallel}| \leq K \\ 0 & \text{if } |k_{\parallel}| > K, \end{cases} \quad (5)$$

and

$$P_{yy}(\mathbf{k}) = \frac{1}{4\pi K} k_x^2 A(k_{\perp}) \begin{cases} 1 & \text{if } |k_{\parallel}| \leq K \\ 0 & \text{if } |k_{\parallel}| > K. \end{cases} \quad (6)$$

In the model described here, we used the (axisymmetric) spectrum $A(k_{\perp})$ and the parameter K which cuts off the spectrum in the parallel direction. Compared to the tensor discussed in Ruffolo & Matthaeus (2013), we have different prefactors in our model because we use a different form of the Fourier transform. As in Ruffolo & Matthaeus (2013) we only consider the special case of axisymmetric turbulence where the spectrum depends only on k_{\perp} . We want to emphasize that $\delta B_z = 0$ in the model considered here and therefore $P_{zz} = 0$. Before we discuss the spectrum $A(k_{\perp})$ we briefly think about the normalization. Since we have to satisfy

$$\begin{aligned} \delta B^2 &= \delta B_x^2 + \delta B_y^2 \\ &= \int d^3k [P_{xx}(\mathbf{k}) + P_{yy}(\mathbf{k})] \\ &= \int_0^{\infty} dk_{\perp} k_{\perp}^3 A(k_{\perp}), \end{aligned} \quad (7)$$

we can determine the constants in the spectrum $A(k_{\perp})$.

³ Equations (1) and (3) look very similar. However, the term (Equation (4)) in UNLT theory is completely different from the corresponding term in NLGC theory. Therefore, we expect that at least in certain limits, the two theories provide very different solutions.

3.2. The Spectrum $A(k_\perp)$

A key element in theories for particle transport and FLRW is the turbulence spectrum. The large scales (corresponding to small wavenumbers) of the spectrum control the field line diffusion coefficients and perpendicular diffusion coefficients of energetic particles (see, e.g., Shalchi & Kourakis 2007; Shalchi & Weinhorst 2009; Minnie et al. 2009; Shalchi et al. 2010). In the following, we use exactly the spectrum proposed by Ruffolo & Matthaeus (2013), which has the form

$$A(k_\perp) = \frac{A_0}{[1 + (k_\perp l_\perp)^2]^{7/3}}. \quad (8)$$

Here we used the characteristic length scale l_\perp which denotes the turnover from the energy range of the spectrum to the inertial range. Therefore, the latter scale is also known as the bendover scale. Usually this scale is directly proportional to the integral scale of the turbulence (see, e.g., Shalchi 2014). By using the normalization condition (Equation (7)), we can specify the parameter A_0 :

$$\delta B^2 = A_0 \int_0^\infty dk_\perp \frac{k_\perp^3}{[1 + (k_\perp l_\perp)^2]^{7/3}}. \quad (9)$$

The latter integral can be solved (see, e.g., Gradshteyn & Ryzhik 2000), and it yields $9/8$. Therefore, one can easily determine the parameter A_0 , and the spectrum (Equation (8)) becomes

$$A(k_\perp) = \frac{8}{9} l_\perp^4 \delta B^2 \frac{1}{[1 + (k_\perp l_\perp)^2]^{7/3}}. \quad (10)$$

With Equation (5) we now know the xx -component of the correlation tensor which enters Equations (1) and (3). Our turbulence model is now complete and, in Section 4, we will use it to compute the perpendicular diffusion coefficient.

3.3. Relation to the Two-dimensional Model

The NRMHD model can be seen as an extension/generalization of the pure 2D model which was often used before in the literature (see, e.g., Fyfe & Montgomery 1976; Fyfe et al. 1977). The pure 2D model is sometimes called the reduced MHD model (see, e.g., Strauss 1976; Montgomery 1982; Higdon 1984). Some aspects of the corresponding spectrum are discussed in Matthaeus et al. (2007) and Shalchi & Weinhorst (2009).

In analytical treatments of turbulence, random walking magnetic field lines, and perpendicular transport of energetic particles, physical quantities are usually given as a wavenumber integral. Let us assume that we have an analytical theory for the quantity ξ_{xx} given as

$$\xi_{xx} = \int d^3k P_{xx}(\mathbf{k}) \chi(k_\parallel, k_\perp). \quad (11)$$

Examples are the NLGC theory (Equation (1)), the UNLT theory (Equation (3)), and the normalization condition (Equation (7)). Now we evaluate the latter form using the NRMHD model (Equation (5)). In this case, we find

$$\xi_{xx}(K) = \frac{1}{4K} \int_{-K}^{+K} dk_\parallel \int_0^\infty dk_\perp k_\perp^3 A(k_\perp) \chi(k_\parallel, k_\perp). \quad (12)$$

Now we consider the limit

$$\xi_{xx}^{2D} := \lim_{K \rightarrow 0} \xi_{xx}(K) \quad (13)$$

Table 1
The Functions $U(k_\perp)$ and $V(k_\perp)$ for NLGC and UNLT Theories

Parameter	NLGC Theory	UNLT Theory
$U(k_\perp)$	$\kappa_\perp k_\perp^2 + v/\lambda_\parallel$	$(4/3)\kappa_\perp k_\perp^2 + v/\lambda_\parallel$
$V(k_\perp)$	κ_\parallel	$v^2/(3\kappa_\perp k_\perp^2)$

and we obtain

$$\xi_{xx}^{2D} = \frac{1}{2} \int_0^\infty dk_\perp k_\perp^3 A(k_\perp) \chi(k_\parallel = 0, k_\perp). \quad (14)$$

The pure 2D model is defined as

$$P_{xx}(\mathbf{k}) = g^{2D}(k_\perp) \frac{\delta(k_\parallel)}{k_\perp} \frac{k_y^2}{k_\perp^2}. \quad (15)$$

Using this model with the form (Equation (11)) we obtain

$$\xi_{xx}^{2D} = \pi \int_0^\infty dk_\perp g^{2D}(k_\perp) \chi(k_\parallel = 0, k_\perp). \quad (16)$$

The latter form can be compared with Equation (14) to find the correspondence

$$g^{2D}(k_\perp) = \frac{1}{2\pi} k_\perp^3 A(k_\perp). \quad (17)$$

Obviously the spectrum $A(k_\perp)$ is directly related to the spectrum used in the pure 2D turbulence model $g^{2D}(k_\perp)$. By combining the latter relation with the spectrum (Equation (10)), one can easily show that this spectrum is a special case of the Shalchi & Weinhorst (2009) model if we set $s = 5/3$ and $q = 3$ therein.

4. COMPUTING THE PERPENDICULAR DIFFUSION COEFFICIENT

In the following, we compute the perpendicular diffusion coefficient based on the two theories discussed in Section 2. Equations (1) and (3) have the form

$$\kappa_\perp = \frac{a^2 v^2}{3B_0^2} \int d^3k \frac{P_{xx}(\mathbf{k})}{U(k_\perp) + V(k_\perp) k_\parallel^2}, \quad (18)$$

where the functions $U(k_\perp)$ and $V(k_\perp)$ are different for the two considered theories. They are summarized in Table 1. With Equation (5) this becomes

$$\begin{aligned} \kappa_\perp &= \frac{a^2 v^2}{3B_0^2} \frac{1}{2K} \\ &\times \int_0^\infty dk_\perp k_\perp^3 A(k_\perp) \frac{\arctan(K\sqrt{V/U})}{\sqrt{UV}}. \end{aligned} \quad (19)$$

Here we kept the spectrum $A(k_\perp)$ in the equation for the perpendicular diffusion coefficient. Later we will replace it by the form (Equation (10)). One can very easily consider the limit $K \rightarrow 0$ and by using $\arctan(x) \approx x$, one can derive the corresponding integral equation for 2D turbulence from Equation (19).

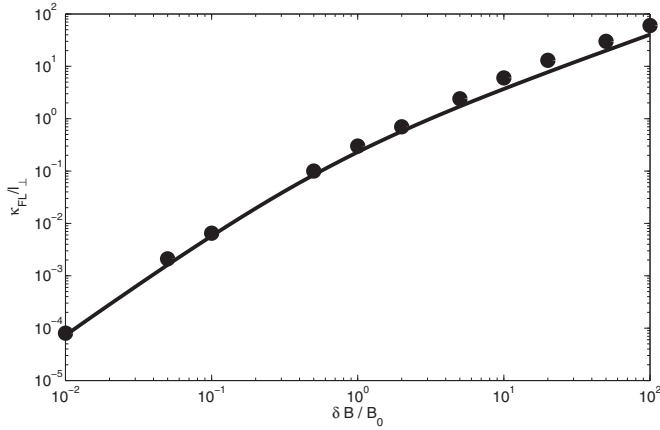


Figure 1. Field line diffusion coefficient for NRMHD turbulence. Shown is $\kappa_{\text{FL}}/l_{\perp}$ vs. the magnetic field ratio $\delta B/B_0$ for $\tilde{K} \equiv Kl_{\perp} = 1$. The solid line represents the analytical result obtained by solving Equation (23) numerically and the dots represent the simulations (see Section 5 for details). We want to emphasize that the solid line is in agreement with the result obtained by Ruffolo & Matthaeus (2013).

4.1. The FLRW Limit from UNLT Theory

One strength of the UNLT theory is that the correct FLRW limit can be derived from it. We demonstrate this for the turbulence model considered here. We can obtain the FLRW limit by suppressing parallel diffusion and by forcing the particle to follow magnetic field lines. This means that we have to set $a^2 = 1$ and $v/\lambda_{\parallel} = 0$ in Equation (19) and in the functions U and V listed in Table 1. Therefore, we have $U = (4/3)\kappa_{\perp}k_{\perp}^2$ and, thus, $\sqrt{U/V} = 2v/3$ and $\sqrt{V/U} = v/(2\kappa_{\perp}k_{\perp}^2)$. With these relations, Equation (19) becomes

$$\kappa_{\perp} = \frac{v}{4KB_0^2} \int_0^{\infty} dk_{\perp} k_{\perp}^3 A(k_{\perp}) \arctan\left(\frac{vK}{2\kappa_{\perp}k_{\perp}^2}\right). \quad (20)$$

The latter equation has the solution

$$\kappa_{\perp} = \frac{v}{2}\kappa_{\text{FL}}, \quad (21)$$

or, in terms of mean free paths,

$$\lambda_{\perp} = \frac{3}{2}\kappa_{\text{FL}}, \quad (22)$$

with the field line diffusion coefficient

$$\kappa_{\text{FL}} = \frac{1}{2KB_0^2} \int_0^{\infty} dk_{\perp} k_{\perp}^3 A(k_{\perp}) \arctan\left(\frac{K}{\kappa_{\text{FL}}k_{\perp}^2}\right). \quad (23)$$

Equations (21) and (22) correspond to the FLRW limit and Equation (23) agrees perfectly with Equation (25) of Ruffolo & Matthaeus (2013). We want to emphasize that Equation (23) was derived from Equation (3), representing the UNLT theory by setting $a^2 = 1$ and $v/\lambda_{\parallel} = 0$ therein. In Ruffolo & Matthaeus (2013), the same result was obtained by employing the field line diffusion theory of Matthaeus et al. (1995). As shown here the UNLT theory of Shalchi (2010) allows the perpendicular diffusion of energetic particles as well as the diffusion of magnetic field lines to be described. In Figure 1, we show the numerical solution of Equation (23). In the latter figure we also show simulations of FLRW confirming the validity of Equation (23). More details about this numerical work can be found in Section 5.

4.2. The Limit $K \rightarrow 0$

The UNLT theory represented by Equation (3) is a special case of the form (Equation (11)) with $\xi_{xx} = \kappa_{xx} = \kappa_{\perp}$ and

$$\chi(k_{\parallel}, k_{\perp}) = \frac{a^2 v^2}{3B_0^2} \frac{1}{F(k_{\parallel}, k_{\perp}) + (4/3)\kappa_{\perp}k_{\perp}^2 + v/\lambda_{\parallel}}, \quad (24)$$

with the function $F(k_{\parallel}, k_{\perp})$ defined in Equation (4). According to Equation (16) this becomes, in the limit $K \rightarrow 0$,

$$\kappa_{\perp} = \frac{\pi}{3} \frac{a^2 v^2}{B_0^2} \int_0^{\infty} dk_{\perp} \frac{g^{2D}(k_{\perp})}{(4/3)\kappa_{\perp}k_{\perp}^2 + v/\lambda_{\parallel}} \quad (25)$$

corresponding to Equation (4) of Shalchi (2013b). The spectrum $g^{2D}(k_{\perp})$ is related to $A(k_{\perp})$ via Equation (17) of the present paper. Therefore, in the limit $K \rightarrow 0$, we expect to find the results derived earlier for 2D turbulence. We want to emphasize that strictly pure 2D turbulence should be considered to be a singular case and that diffusion theories such as NLGC and UNLT theories are no longer valid for that specific model of turbulence.

4.3. Perpendicular Diffusion for the General Case

Here we return to the general form (Equation (19)) with the functions $U(k_{\perp})$ and $V(k_{\perp})$ from Table 1. Equation (19) has to be evaluated numerically. Therefore, we introduce new quantities which are more appropriate for numerical treatments of the transport. In the following we use

$$\begin{aligned} \tilde{K} &= l_{\perp} K, \\ S &= K \sqrt{V/U}, \\ Q &= \frac{1}{v} \sqrt{U/V}, \end{aligned} \quad (26)$$

and instead of using the spatial diffusion coefficient we use the mean free paths defined as $\lambda_{\parallel} = 3\kappa_{\parallel}/v$ and $\lambda_{\perp} = 3\kappa_{\perp}/v$. By using the latter parameters, Equation (19) becomes

$$\frac{\lambda_{\perp}}{l_{\perp}} = \frac{a^2}{2\tilde{K}B_0^2} \int_0^{\infty} dk_{\perp} k_{\perp}^3 A(k_{\perp}) \frac{\arctan[S(k_{\perp})]}{Q(k_{\perp})}, \quad (27)$$

where the parameters/functions S and Q can be found below. To proceed we employ the spectrum (Equation (10)) and we use the integral transformation $x = l_{\perp} k_{\perp}$ to obtain

$$\frac{\lambda_{\perp}}{l_{\perp}} = \frac{4a^2 \delta B^2}{9\tilde{K} B_0^2} \int_0^{\infty} dx \frac{x^3}{(1+x^2)^{7/3}} \frac{\arctan[S(x)]}{Q(x)}. \quad (28)$$

The two functions $S(x)$ and $Q(x)$ are different for the NLGC and UNLT theories. For the NLGC theory we have to use

$$S_N(x) = \tilde{K} \sqrt{\left(\frac{\lambda_{\parallel}}{3l_{\perp}}\right) / \left(\frac{\lambda_{\perp}}{3l_{\perp}}x^2 + \frac{l_{\perp}}{\lambda_{\parallel}}\right)} \quad (29)$$

and

$$Q_N(x) = \sqrt{\left(\frac{\lambda_{\perp}}{3l_{\perp}}x^2 + \frac{l_{\perp}}{\lambda_{\parallel}}\right) \frac{\lambda_{\parallel}}{3l_{\perp}}}. \quad (30)$$

For the UNLT theory, however, we have

$$S_U(x) = \tilde{K} \sqrt{\left(\frac{l_{\perp}}{\lambda_{\perp}x^2}\right) / \left(\frac{4\lambda_{\perp}}{9l_{\perp}}x^2 + \frac{l_{\perp}}{\lambda_{\parallel}}\right)} \quad (31)$$

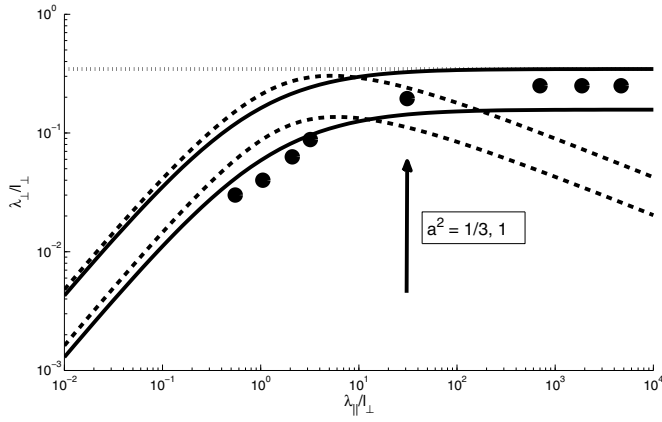


Figure 2. Perpendicular mean free path vs. the parallel mean free path for the NRMHD model. We compare the NLGC theory (dashed line) with the UNLT theory (solid line), and the field line random walk limit (dotted line). Here we set $\tilde{K} = 1$ and $\delta B^2/B_0^2 = 1$. The dots represent the test-particle simulations discussed in Section 5. The two analytical theories were evaluated for two different values of the parameter a .

and

$$Q_U(x) = \sqrt{\frac{4}{9} + \frac{l_\perp^2}{\lambda_\parallel \lambda_\perp x^2}}. \quad (32)$$

In the following, we compute the perpendicular mean free path versus the parallel mean free path for different values of the parameters a^2 , $\delta B^2/B_0^2$, and \tilde{K} . The values used are listed in the caption of the corresponding figure. By specifying these parameters we can solve Equation (28) for the NLGC theory and the UNLT theory numerically.

In Figure 2, we compute the perpendicular mean free path versus the parallel mean free path for two different values of the parameter a^2 and $\tilde{K} = 1$ and $\delta B^2/B_0^2 = 1$. Also shown are the test-particle simulations which are discussed in Section 5. We can easily see that for NRMHD turbulence, there are two regimes. In the regime $\lambda_\parallel \ll l_\perp$ the perpendicular mean free path increases linearly with the parallel mean free path. In this regime, the NLGC and UNLT theories provide very similar results. We will discuss below that this similarity cannot be found in the general case. As soon as the parallel mean free path becomes longer than the bendover scale l_\perp , the two theories provide very different results. Whereas the perpendicular mean free path obtained from NLGC theory decreases with increasing λ_\parallel , the UNLT provides a perpendicular mean free path which becomes constant. In the case $\lambda_\parallel \gg l_\perp$, the results obtained from UNLT theory are very close to the FLRW limit $\lambda_\perp = 3\kappa_{\text{FL}}/2$. In Appendix A we consider the limit $\lambda_\parallel \rightarrow \infty$ in the NLGC theory. We show there that in this limit we find $\lambda_\perp \sim \lambda_\parallel^{-1/3}$, in disagreement with the UNLT theory and simulations.⁴

In Figures 3 and 4, we study the influence of the two parameters $\delta B/B_0$ and \tilde{K} on the perpendicular diffusion coefficient. For small $\tilde{K} \rightarrow 0$ the perpendicular mean free path approaches the result one would obtain for 2D turbulence whereas for larger values of \tilde{K} the perpendicular mean free path is getting shorter.

⁴ We want to point out that we indeed find the exponent $-1/3$ for the dependence on the parallel mean free path. In Shalchi et al. (2004), for instance, $\lambda_\perp \sim \lambda_\parallel^{+1/3}$ was derived, which is different from the result derived in the present paper. The exponent $+1/3$ was derived for pure 2D turbulence and a very specific spectrum. Therefore, this result has nothing to do with the exponent we derived in the current paper.

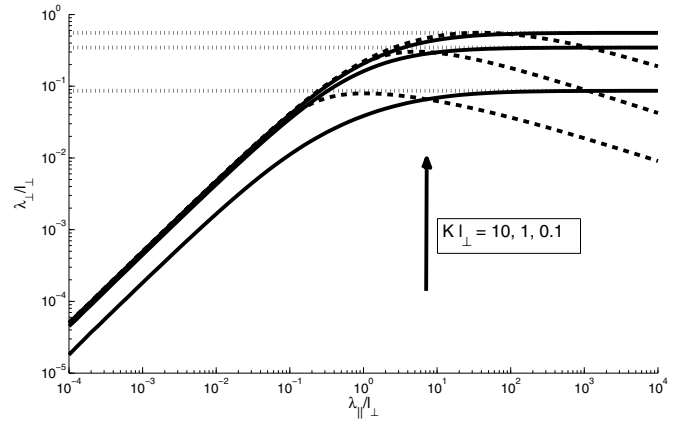


Figure 3. Perpendicular mean free path vs. the parallel mean free path for the NRMHD model. We compare the NLGC theory (dashed line) with the UNLT theory (solid line), and the field line random walk limit (dotted line). We compute λ_\perp for $\tilde{K} = Kl_\perp = 10, 1, 0.1$. Here we set $a^2 = 1$ and $\delta B^2/B_0^2 = 1$.

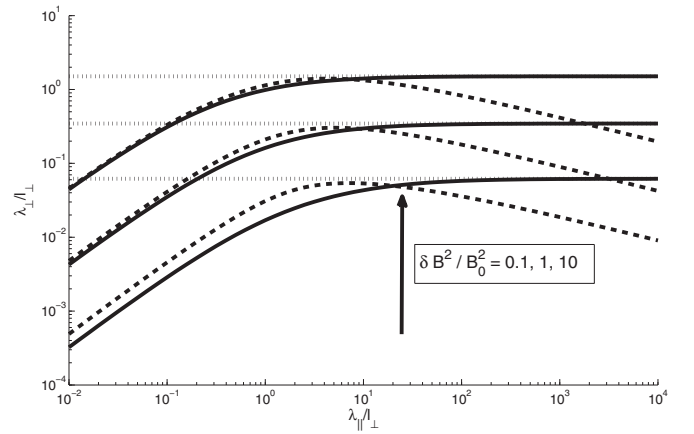


Figure 4. Perpendicular mean free path vs. the parallel mean free path for the NRMHD model. We compare the NLGC theory (dashed line) with the UNLT theory (solid line), and the field line random walk limit (dotted line). We compute λ_\perp for $\delta B^2/B_0^2 = 0.1, 1, 10$. Here we set $a^2 = 1$ and $\tilde{K} = 1$.

For such large values of \tilde{K} , Figure 3 also shows a further discrepancy between NLGC and UNLT theories. For $\tilde{K} = 10$ the two theories disagree with each other even if the parallel mean free path is very short. NLGC theories predict that the ratio $\lambda_\perp/\lambda_\parallel$ does not depend on the parameter \tilde{K} (see Appendix A) whereas UNLT theory clearly states a dependence on this parameter. This discrepancy is a subject for future work and therewith analytical solutions of the UNLT integral equation for NRMHD turbulence. From Figure 4, one can see that the perpendicular mean free path depends sensitively on the magnetic field ratio $\delta B/B_0$. For weak turbulence amplitudes such as $\delta B^2/B_0^2 = 0.1$, we find again a discrepancy between NLGC and UNLT theories. Obviously, these two theories provide different results for most turbulence and particle parameters.

We want to emphasize that all our results were obtained for a specific spectrum, namely, the model spectrum given by Equation (10), which is the spectrum proposed by Ruffolo & Matthaeus (2013). For a different spectrum (e.g., a different spectral index in the energy range, a spectrum with cut-off at small wavenumbers) one could obtain different results and the differences between NLGC and UNLT theories could be smaller or larger in such cases.

Table 2
Simulated Field Line Diffusion Coefficient for the NRMHD
Model Versus the Ratio $\delta B/B_0$

$\delta B/B_0$	0.01	0.05	0.1	0.5	1.0	2.0	5.0	10.0	20.0	50.0	100.0
κ_{FL}/l_\perp	8.0×10^{-5}	0.0021	0.0065	0.1	0.3	0.7	2.4	6.0	13.0	30.0	60.0

Note. For all simulation runs we set $\tilde{K} = 1.0$.

Table 3
Simulated Mean Free Paths Along and Across the Mean Magnetic Field
Versus the Dimensionless Magnetic Rigidity R_L/l_\perp

R_L/l_\perp	0.001	0.01	0.05	0.1	1.0	5.0	10.0	16.0	20.0
$\lambda_\parallel/l_\perp$	0.55	1.05	2.1	3.2	31	700	1875	4700	1.1×10^4
λ_\perp/l_\perp	0.03	0.04	0.063	0.088	0.195	0.25	0.25	0.25	0.25

Note. Here we have used $\tilde{K} = 1.0$ and $\delta B^2/B_0^2 = 1.0$.

5. SIMULATIONS

A powerful tool in order to test analytical theories such as NLGC or UNLT theories are test-particle simulations. In the current section, we use an extension of the code used in Hussein & Shalchi (2014). In the following, we discuss some technical details of that code, the results obtained for the field line diffusion coefficient, and the simulated parallel and perpendicular diffusion coefficients.

5.1. The Test-particle Code

Test-particle simulations have been performed before. In Hussein & Shalchi (2014), for instance, we used a code to simulate the interaction between energetic particles and different turbulence models. These models were the slab model, the isotropic model, and a composition of slab and 2D models. In all these models only one independent wavevector component controls the turbulent magnetic field. The NRMHD model considered here is more complicated because two components are relevant, namely k_\parallel and k_\perp . Therefore, one has to evaluate an extra sum numerically, making the simulations much more time-consuming. We describe the technical details of our numerical tool in Appendix B and focus on the results in the main part of this paper.

5.2. The Field Line Diffusion Coefficient

By solving the field line equation $dx = dz\delta B_x/B_0$ numerically, one can obtain the field line diffusion coefficient for different parameter values. Here we set $\tilde{K} = 1$ and compute the field line diffusion coefficient for different values of the magnetic field ratio $\delta B/B_0$. The results are listed in Table 2 and they are compared with the analytical results in Figure 1. As shown in the latter figure, the agreement between analytical theory and simulations is very good, confirming the nonlinear theory for field line diffusion developed by Matthaeus et al. (1995) and the UNLT theory of Shalchi (2010). Our simulations for random walking magnetic field lines agree well with the simulations presented in Snodin et al. (2013).

5.3. The Particle Diffusion Coefficients

In the current paragraph, we use the code described above to compute the parallel and perpendicular mean free paths. For these simulations we set $\tilde{K} = 1$ and $\delta B/B_0 = 1$. Our results are listed in Table 3 and they are visualized in Figure 2. It is shown

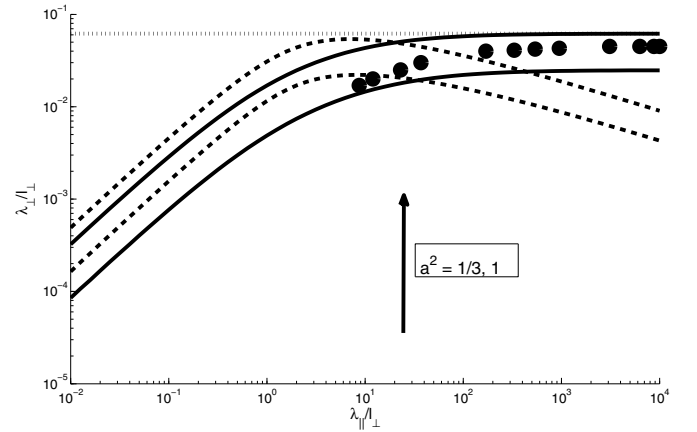


Figure 5. Perpendicular mean free path vs. the parallel mean free path for the NRMHD model. We compare the NLGC theory (dashed line) with the UNLT theory (solid line), and the field line random walk limit (dotted line). Here we set $\tilde{K} = 1$ and $\delta B^2/B_0^2 = 0.1$. The dots represent the simulations.

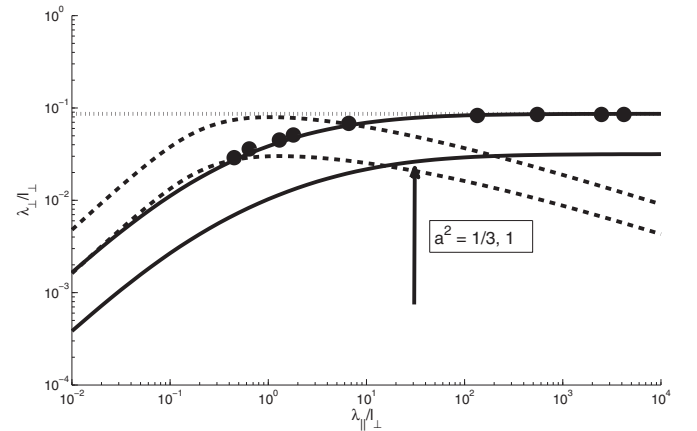


Figure 6. Perpendicular mean free path vs. the parallel mean free path for the NRMHD model. We compare the NLGC theory (dashed line) with the UNLT theory (solid line), and the field line random walk limit (dotted line). Here we set $\tilde{K} = 10$ and $\delta B^2/B_0^2 = 1.0$. The dots represent the simulations.

Table 4
Simulated Mean Free Paths Along and Across the Mean Magnetic Field
Versus the Dimensionless Magnetic Rigidity R_L/l_\perp

R_L/l_\perp	0.005	0.01	0.05	0.1	1.0	5.0	10.0	20.0	25.0
$\lambda_\parallel/l_\perp$	0.45	0.64	1.3	1.8	6.6	135	550	2480	4200
λ_\perp/l_\perp	0.029	0.036	0.045	0.051	0.068	0.083	0.085	0.085	0.085

Note. Here we have used $\tilde{K} = 10$ and $\delta B^2/B_0^2 = 1.0$.

that the numerical perpendicular mean free path agrees well with the NLGC and UNLT theories for the case of small parallel mean free paths. For long parallel mean free paths, however, only the UNLT theory agrees with the simulations. The decreasing perpendicular mean free path for larger values of λ_\parallel provided by the NLGC theory cannot be seen in the simulations. The prediction of the UNLT theory that the perpendicular mean free path approaches asymptotically the FLRW limit, in contrast, can also be seen in the numerical work. Therefore, the UNLT theory is confirmed once again.

In Figures 5 and 6, we repeat the simulations for $\tilde{K} = 1$, $\delta B^2/B_0^2 = 0.1$ and $\tilde{K} = 10$, $\delta B^2/B_0^2 = 1.0$, respectively. The results are listed in Tables 4 and 5. Qualitatively, the results are very similar compared to the previous run. We can see that

Table 5Simulated Mean Free Paths Along and Across the Mean Magnetic Field Versus the Dimensionless Magnetic Rigidity R_L/l_\perp

R_L/l_\perp	0.005	0.01	0.05	0.1	1.0	2.0	3.0	5.0	10.0	20.0	25.0	30.0
$\lambda_\parallel/l_\perp$	8.7	12	23	37	170	330	540	950	3100	6300	8750	10^4
λ_\perp/l_\perp	0.017	0.02	0.025	0.03	0.04	0.041	0.042	0.043	0.045	0.045	0.045	0.045

Note. Here we have used $\tilde{K} = 1.0$ and $\delta B^2/B_0^2 = 0.1$.

now even for small values of λ_\parallel , the NLGC and UNLT theories disagree with each other. The simulations clearly support the UNLT theory. It seems, however, that the parameter a^2 depends on the values of \tilde{K} and $\delta B^2/B_0^2$. More investigations concerning the value of a^2 have to be done in the future.

6. SUMMARY AND CONCLUSION

In Ruffolo & Matthaeus (2013) the model of NRMHD turbulence was proposed and used to compute the diffusion coefficient of random walking magnetic field lines based on the nonlinear diffusion theory of Matthaeus et al. (1995). In this paper, we investigated the perpendicular diffusion of energetic particles by using two analytical theories, namely, the NLGC theory of Matthaeus et al. (2003) and the UNLT theory of Shalchi (2010). Furthermore, we performed test-particle simulations to obtain field line diffusion and particle transport coefficients. We obtained the following result.

1. We showed that the FLRW limit with the correct field line diffusion coefficient can be obtained from the UNLT theory in the appropriate limit. For the case of NRMHD turbulence the field line diffusion coefficient already obtained by Ruffolo & Matthaeus (2013) is derived from UNLT theory. Our test-particle simulations confirm these previous results and therewith our current understanding of field line diffusion (see Figure 1).
2. We obtained for the first time the perpendicular diffusion coefficient of energetic particles for NRMHD turbulence. We showed how the two parameters $\tilde{K} = Kl_\perp$ and $\delta B/B_0$ influence the perpendicular mean free path. The UNLT and NLGC theories provide very different results for the turbulence model considered here (see Figures 2, 5, and 6 of the current paper). According to the UNLT theory the perpendicular mean free path increases linearly with the parallel mean free path λ_\parallel and in the limit of large λ_\parallel it becomes independent of the latter parameter. This behavior was already found for other turbulence models and agrees with the universality of the transport discussed in detail in Shalchi (2014).
3. We tested the validity of the NLGC and UNLT theories by comparing them with test-particle simulations. As shown in Figures 2, 5, and 6, only the UNLT theory agrees with the simulations for NRMHD turbulence. The scaling $\lambda_\perp \sim \lambda_\parallel^{-1/3}$ predicted by the NLGC theory for long parallel mean free paths cannot be seen in the simulations. Furthermore, we also find that for a short parallel mean free path, the NLGC theory predicts that the ratio $\lambda_\perp/\lambda_\parallel$ does not depend on the parameter \tilde{K} whereas UNLT shows a clear dependence.

The UNLT theory originally developed by Shalchi (2010) can correctly describe field line diffusion and perpendicular transport of energetic particles in NRMHD turbulence. This work, therefore, also complements previous work that has shown

that the UNLT theory can accurately describe transport in two-component turbulence and Goldreich–Sridhar turbulence (see, e.g., Tautz & Shalchi 2011; Shalchi 2013a). It will be subject of future work to derive analytical forms for the perpendicular diffusion coefficient in NRMHD turbulence based on the UNLT theory.

M.H. and A.S. acknowledge support by the Natural Sciences and Engineering Research Council (NSERC) of Canada and national computational facility provided by WestGrid. We are also grateful to S. Safi-Harb for providing her CFI-funded computational facilities for code tests and for some of the simulation runs presented here.

APPENDIX A

ASYMPTOTIC LIMITS DERIVED FROM THE NLGC INTEGRAL EQUATION

Here we explore the asymptotic limits one can obtain from the NLGC theory. A more detailed discussion of such limits and the corresponding limits obtained from the UNLT theory can be found in the main part of the text.

A.1. The Limit $\lambda_\parallel \rightarrow 0$

Here we consider the (formal) limit $\lambda_\parallel \rightarrow 0$ in the NLGC integral equation. In this limit Equations (29) and (30) provide

$$\begin{aligned} S(x) &\rightarrow \frac{\tilde{K}\lambda_\parallel}{\sqrt{3}l_\perp} \rightarrow 0, \\ Q(x) &\rightarrow \frac{1}{\sqrt{3}}, \end{aligned} \quad (\text{A1})$$

and, therefore,

$$\arctan(S) \rightarrow S. \quad (\text{A2})$$

With the latter three limits, Equation (28) becomes

$$\frac{\lambda_\perp}{l_\perp} = \frac{4a^2 \delta B^2}{9\tilde{K} B_0^2} \frac{\tilde{K}\lambda_\parallel}{l_\perp} \int_0^\infty dx \frac{x^3}{(1+x^2)^{7/3}}. \quad (\text{A3})$$

The x -integral can be solved by (see, e.g., Gradshteyn & Ryzhik 2000)

$$\int_0^\infty dx \frac{x^3}{(1+x^2)^{7/3}} = \frac{9}{8}. \quad (\text{A4})$$

Therewith Equation (A3) becomes

$$\frac{\lambda_\perp}{\lambda_\parallel} = \frac{a^2 \delta B^2}{2 B_0^2} \quad (\text{A5})$$

which was derived before for 2D turbulence (see, e.g., Shalchi et al. 2004).

A.2. The Limit $\lambda_{\parallel} \rightarrow \infty$

Here we investigate the limit $\lambda_{\parallel} \rightarrow \infty$ in the NLGC integral equation. In this limit Equations (29) and (30) provide

$$\begin{aligned} S(x) &\rightarrow \frac{\tilde{K}}{x} \sqrt{\frac{\lambda_{\parallel}}{\lambda_{\perp}}} \rightarrow \infty, \\ Q(x) &\rightarrow \frac{\sqrt{\lambda_{\parallel}\lambda_{\perp}}}{3l_{\perp}} x, \end{aligned} \quad (\text{A6})$$

and, therefore,

$$\arctan(S) \rightarrow \pi/2. \quad (\text{A7})$$

With the latter three limits, Equation (28) becomes

$$\frac{\lambda_{\perp}}{l_{\perp}} = \frac{2\pi a^2 \delta B^2}{3\tilde{K} B_0^2} \frac{l_{\perp}}{\sqrt{\lambda_{\parallel}\lambda_{\perp}}} \int_0^{\infty} dx \frac{x^2}{(1+x^2)^{7/3}}. \quad (\text{A8})$$

The x -integral can be solved by (see, e.g., Gradshteyn & Ryzhik 2000)

$$\int_0^{\infty} dx \frac{x^2}{(1+x^2)^{7/3}} = \frac{\sqrt{\pi}}{4} \frac{\Gamma(5/6)}{\Gamma(7/3)}, \quad (\text{A9})$$

where we used the *gamma function* $\Gamma(z)$. Therewith Equation (A8) becomes

$$\frac{\lambda_{\perp}}{l_{\perp}} = \frac{\pi^{3/2} a^2 \Gamma(5/6) \delta B^2}{6\tilde{K} \Gamma(7/3) B_0^2} \frac{l_{\perp}}{\sqrt{\lambda_{\parallel}\lambda_{\perp}}}. \quad (\text{A10})$$

The latter equations can easily be solved by

$$\frac{\lambda_{\perp}}{l_{\perp}} = \left[\frac{\pi^{3/2} a^2 \Gamma(5/6) \delta B^2}{6\tilde{K} \Gamma(7/3) B_0^2} \right]^{2/3} \left(\frac{l_{\perp}}{\lambda_{\parallel}} \right)^{1/3}. \quad (\text{A11})$$

A more detailed discussion of the latter formula can be found in Section 4.3.

APPENDIX B

TECHNICAL DETAILS OF THE TEST-PARTICLE SIMULATIONS

In order to calculate the turbulent magnetic field at the position of the charged particle, one can use the Fourier representation

$$\delta \mathbf{B}(\mathbf{x}) = \int d^3k \delta \mathbf{B}(\mathbf{k}) e^{i\mathbf{k} \cdot \mathbf{x}}. \quad (\text{B1})$$

In numerical treatments of test-particle transport, the three-dimensional wavenumber integral has to be replaced by sums. In turbulence models with reduced dimensionality, such as slab or 2D models, and for isotropic turbulence, this integral can be replaced by a single sum. For the NRMHD model considered in the present paper, however, we have to use two sums. Therefore, the turbulent magnetic field at the particle position is given by

$$\begin{aligned} \delta \mathbf{B}(x, y, z) &= \text{Re} \sum_{m=1}^{N_m} \sum_{n=1}^{N_n} \text{Amp}(k_n, k_m) \hat{\xi}_n \\ &\quad \times \exp[i(k_n y'_n + k_m z_m + \beta_n)]. \end{aligned} \quad (\text{B2})$$

Here we used the polarization vector

$$\hat{\xi}_n = \begin{pmatrix} -\sin \phi_n \\ \cos \phi_n \\ 0 \end{pmatrix}, \quad (\text{B3})$$

where we ensured that $\delta B_z = 0$. The coordinates x'_n and y'_n are obtained from a 2D rotational matrix whose azimuthal angles, ϕ_n , are randomly generated for each summand n due to symmetry reasons:

$$\begin{pmatrix} x'_n \\ y'_n \end{pmatrix} = \begin{pmatrix} -\sin \phi_n & \cos \phi_n \\ \cos \phi_n & \sin \phi_n \end{pmatrix} \begin{pmatrix} x \\ y \end{pmatrix}. \quad (\text{B4})$$

In Equation (B2), $\text{Amp}(k_n, k_m) = \text{Amp}(k_{\perp}, k_{\parallel})$ represents the wave amplitude associated with mode n and m . Moreover, k_n and k_m stands for the wavenumbers in the perpendicular and parallel directions, respectively. β_n is just a random plane wave phase. Basically, the NRMHD model is a broadened 2D model, where the parallel component is added to the pure perpendicular component. Therefore, the model explained above is the same as used in Hussein & Shalchi (2014) by setting $\theta_n = \alpha_n = \pi/2$ and adding the parallel contribution separately.

The wave amplitude $\text{Amp}(k_n, k_m)$ introduced above reads

$$\text{Amp}^2(k_n, k_m) = \frac{G(k_n) \Delta k_m \Delta k_n}{\sum_{\mu=1}^{N_m} \sum_{\nu=1}^{N_n} G(k_{\nu}) \Delta k_{\mu} \Delta k_{\nu}} \quad (\text{B5})$$

and the spectrum $G(k_n)$ is defined as

$$G(k_n) = \frac{(k_n l_{\perp})^q}{[1 + (k_n l_{\perp})^2]^{(s+q)/2}}. \quad (\text{B6})$$

As in analytical treatments, we used the energy range spectral index q and inertial spectral index s , respectively. For these two parameters we use $q = 3$ and $s = 5/3$ as explained in the main part of the paper. Δk_m and Δk_n are the spacings between wavenumbers, where a logarithmic spacing in k_m and k_n is implemented so that $\Delta k_m/k_m$ and $\Delta k_n/k_n$ are constant via the relation

$$\frac{\Delta k_n}{k_n} = \exp \left[\frac{\ln(k_{n,\max}/k_{n,\min})}{N_n - 1} \right] \quad (\text{same in } m). \quad (\text{B7})$$

We should note here that $k_{m,\max} = \tilde{K}$.

The trajectories of 1000 particles were traced to yield the corresponding diffusion coefficients for each simulation run. For the number of modes summed over in parallel and perpendicular directions, the parallel wavenumbers need to be distributed finely enough so that the resonance condition $R_L k_{\parallel} \approx 1$ is satisfied. Here we have used the unperturbed Larmour radius R_L . The way we constructed the NRMHD model in our simulations is so that we started with a 2D turbulence geometry first, which only contains perpendicular wavenumbers extending theoretically until infinity. Then we broadened this model by a parallel portion which has a cut-off value at \tilde{K} . Taking all of that into account and to keep computational time relatively reasonable, we used $N_n = 256$ and $N_m = 32$ for our numerical calculations. It is worth noting that we performed test runs with N_m up to 128 and no significant differences were noticed. The size of the box was restricted by the so-called scaling condition, which ensures that no particle travels beyond the maximum size of the system, $L_{\max} = k_{\min}^{-1}$. This is ensured via the relation $\Omega t_{\max} k_{\min} R_L < 1$, which corresponds to $v t_{\max} < L_{\max}$. In both parallel and perpendicular directions, $k_{\min} = 10^{-5}$, corresponding to a relatively huge box where particles are trapped. Therefore, we ensured that finite box-size effects do not occur. This corresponds to a spectrum without cut-off in analytical treatments of the transport.

REFERENCES

- Alania, M. V., Wawrzynczak, A., Sdobnov, V. E., & Kravtsova, M. V. 2013, [SoPh](#), **286**, 561
- Berkhuijsen, E. M., Beck, R., & Tabatabaei, F. S. 2013, [MNRAS](#), **435**, 1598
- Bieber, J. W., Matthaeus, W. H., Shalchi, A., & Qin, G. 2004, [GeoRL](#), **31**, 10
- Buffie, K., Heesen, V., & Shalchi, A. 2013, [ApJ](#), **764**, 37
- Engelbrecht, N. E., & Burger, R. A. 2013, [ApJ](#), **779**, 158
- Ferrand, G., Danos, R. J., Shalchi, A., et al. 2014, [ApJ](#), **792**, 133
- Fyfe, D., Joyce, G., & Montgomery, D. 1977, [JPIPh](#), **17**, 317
- Fyfe, D., & Montgomery, D. 1976, [JPIPh](#), **16**, 181
- Ghilea, M. C., Ruffolo, D., Chuychai, P., et al. 2011, [ApJ](#), **741**, 16
- Gradshteyn, I. S., & Ryzhik, I. M. 2000, Table of Integrals, Series, and Products (New York: Academic)
- Higdon, J. C. 1984, [ApJ](#), **285**, 109
- Hussein, M., & Shalchi, A. 2014, [ApJ](#), **785**, 31
- Jokipii, J. R. 1966, [ApJ](#), **146**, 480
- Jokipii, J. R., Kóta, J., & Giacalone, J. 1993, [GeoRL](#), **20**, 1759
- Jones, F. C., Jokipii, J. R., & Baring, M. G. 1998, [ApJ](#), **509**, 238
- Li, G., Shalchi, A., Ao, X., Zank, G., & Verkhoglyadova, O. P. 2012, [AdSpR](#), **49**, 1067
- Lynn, J. W., Quataert, E., Chandran, B. D. G., & Parrish, I. J. 2014, [ApJ](#), **791**, 71
- Manuel, R., Ferreira, S. E. S., & Potgieter, M. S. 2014, [SoPh](#), **289**, 2207
- Matthaeus, W. H., Bieber, J. W., Ruffolo, D., Chuychai, P., & Minnie, J. 2007, [ApJ](#), **667**, 956
- Matthaeus, W. H., Gray, P. C., Pontius, D. H., Jr., & Bieber, J. W. 1995, [PhRvL](#), **75**, 2136
- Matthaeus, W. H., Qin, G., Bieber, J. W., & Zank, G. P. 2003, [ApJL](#), **590**, L53
- Minnie, J., Matthaeus, W. H., Bieber, J. W., Ruffolo, D., & Burger, R. A. 2009, [JGRA](#), **114**, A01102
- Montgomery, D. 1982, [PhST](#), **2**, 83
- Potgieter, M. S., Vos, E. E., Boezio, M., et al. 2014, [SoPh](#), **289**, 391
- Qin, G. 2007, [ApJ](#), **656**, 217
- Qin, G., Matthaeus, W. H., & Bieber, J. W. 2002, [GeoRL](#), **29**, 1048
- Ruffolo, D., & Matthaeus, W. H. 2013, [PhPI](#), **20**, 012308
- Ruffolo, D., Pianpanit, T., Matthaeus, W. H., & Chuychai, P. 2012, [ApJL](#), **747**, L34
- Shalchi, A. 2006, [A&A](#), **453**, L43
- Shalchi, A. 2009, Nonlinear Cosmic Ray Diffusion Theories (Astrophysics and Space Science Library, Vol. 362; Berlin: Springer)
- Shalchi, A. 2010, [ApJL](#), **720**, L127
- Shalchi, A. 2013a, [Ap&SS](#), **344**, 187
- Shalchi, A. 2013b, [ApJ](#), **774**, 7
- Shalchi, A. 2014, [AdSpR](#), **53**, 1024
- Shalchi, A., Bieber, J. W., & Matthaeus, W. H. 2004, [ApJ](#), **604**, 675
- Shalchi, A., & Kourakis, I. 2007, [PhPI](#), **14**, 112901
- Shalchi, A., Li, G., & Zank, G. P. 2010, [Ap&SS](#), **325**, 99
- Shalchi, A., & Weinhorst, B. 2009, [AdSpR](#), **43**, 1429
- Snodin, A. P., Ruffolo, D., Oughton, S., Servidio, S., & Matthaeus, W. H. 2013, [ApJ](#), **779**, 56
- Strauss, H. R. 1976, [PhFI](#), **19**, 134
- Tautz, R. C., & Shalchi, A. 2011, [ApJ](#), **735**, 92
- Wang, Y., Qin, G., & Zhang, M. 2012, [ApJ](#), **752**, 37